Inorg. Chem. **2008**, *47*, 2955−2963

Photophysics of Diplatinum Polyynediyl Oligomers: Chain Length Dependence of the Triplet State in sp Carbon Chains

Richard T. Farley,[†] Qinglin Zheng,[‡] John A. Gladysz,[*,‡,§] and Kirk S. Schanze[*,†]

Department of Chemistry, University of Florida, P.O. Box 117200, Gainesville, Florida 32611, Institut für Organische Chemie and Interdisciplinary Center for Molecular Materials, Friedrich-Alexander-Universität Erlangen-Nürnberg, Henkestrasse 42, 91054 Erlangen, Germany, and Department of Chemistry, Texas A&M University, P.O. Box 30012, College Station, Texas 77842

Received June 21, 2007

The series of polyynes with the structure *trans,trans*-[Ar−Pt(P$_2$)−(C≡C)$_n$−Pt(P$_2$)−Ar], where P = tri(*p*-tolyl)phosphine, Ar = *p*-tolyl, and *n* = 3, 4, 5, 6 (6, 8, 10, 12 sp carbon atoms), has been subjected to a comprehensive photophysical investigation. At low temperature (*T* < 140 K) in a 2-methyltetrahydrofuran (MTHF) glass, the complexes exhibit moderately efficient phosphorescence appearing as a series of narrow (fwhm < 200 cm^{-1}) vibronic bands separated by ca. 2100 cm^{-1}. The emission is assigned to a $^3\pi,\pi^*$ triplet state that is concentrated on the sp carbon chain, and the vibronic progression arises from coupling of the excitation to the −C≡C− stretch. The 0−0 energy of the phosphorescence decreases with increasing sp carbon chain length, spanning a range of over 6000 cm^{-1} across the series. Transient absorption spectroscopy carried out at ambient temperature confirms that the $^3\pi,\pi^*$ triplet is produced efficiently, and it displays a strongly allowed triplet−triplet absorption. In the MTHF solvent glass (*T* < 140 K), the emission lifetimes increase with emission energy. Analysis of the triplet nonradiative decay rates reveals a quantitative energy gap law correlation. The nonradiative decay rates can be calculated by using parameters recovered from a single-mode Franck−Condon fit of the emission spectra.

Introduction

Over the past few decades, there has been increasing interest in the study of organic and organometallic oligomers that feature extended carbon chains, e.g., R−(C≡C)$_n$−R and L$_y$M−(C≡C)$_n$−ML$_y$.[1−14] The extended π-systems and preferred linear structure characteristic of these carbon-chain oligomers make them potentially useful as molecular wires for transport of charge (polarons) or excitons on the nanoscale.[15] On a fundamental level, oligoynes are unique in that they provide one of the simplest possible linear

* To whom correspondence should be addressed. Phone: 352-392-9133 (K.S.S.), 979-845-1399 (J.A.G.). Fax: 202-513-8648 (K.S.S.), 979-845-5629 (J.A.G.). E-mail: kschanze@chem.ufl.edu (K.S.S.), gladysz@mail.chem.tamu.edu (J.A.G.).

† University of Florida.

‡ Friedrich-Alexander-Universität Erlangen-Nürnberg.

§ Texas A&M University.

(1) Jones, E. R. H.; Lee, H. H.; Whiting, M. C. *J. Chem. Soc.* **1960**, 3483–3489.

(2) Johnson, T. R.; Walton, D. R. M. *Tetrahedron* **1972**, *28*, 5221–5236.

(3) Eastmond, R.; Walton, D. R. M.; Johnson, T. R. *Tetrahedron* **1972**, *28*, 4601–4616.

(4) Schermann, G.; Grosser, T.; Hampel, F.; Hirsch, A. *Chem.—Eur. J.* **1997**, *3*, 1105–1112.

(5) Gibtner, T.; Hampel, F.; Gisselbrecht, J. P.; Hirsch, A. *Chem.—Eur. J.* **2002**, *8*, 408–432.

(6) Klinger, C.; Vostirowsky, O.; Hirsch, A. *Eur. J. Org. Chem.* **2006**, 1508–1524.

(7) Eisler, S.; Slepkov, A. D.; Elliott, E.; Luu, T.; McDonald, R.; Hegmann, F. A.; Tykwinski, R. R. *J. Am. Chem. Soc.* **2005**, *127*, 2666–2676.

(8) Luu, T.; Elliott, E.; Slepkov, A. D.; Eisler, S.; McDonald, R.; Hegmann, F. A.; Tykwinski, R. R. *Org. Lett.* **2005**, *7*, 51–54.

(9) Dembinski, R.; Bartik, T.; Bartik, B.; Jaeger, M.; Gladysz, J. A. *J. Am. Chem. Soc.* **2000**, *122*, 810–822.

(10) Mohr, W.; Stahl, J.; Hampel, F.; Gladysz, J. A. *Chem.—Eur. J.* **2003**, *9*, 3324–3340.

(11) Zheng, Q.; Bohling, J. C.; Peters, T. B.; Frisch, A. C.; Hampel, F.; Gladysz, J. A. *Chem.—Eur. J.* **2006**, *12*, 6486–6505.

(12) Szafert, S.; Gladysz, J. A. *Chem. Rev.* **2003**, *103*, 4175–4205. **2006**, *106*, PR1PR33.

(13) Paul, F.; Lapinte, C. In *Unusual Structures and Physical Properties in Organometallic Chemistry*; Gielen, M., Willem, R., Wrackmyer, B., Eds.; Wiley: New York, 2002; pp 220–291..

(14) Bruce, M. I.; Low, P. J. *Adv. Organomet. Chem.* **2004**, *50*, 179.

(15) Adams, D.; Brus, L.; Chidsey, C. E. D.; Creager, S.; Creutz, C.; Kagan, C. R.; Kamat, P.; Lieberman, M.; Lindsay, S.; Marcus, R. A.; Metzger, R. M.; Michel-Beyerle, M. E.; Miller, J. R.; Newton, M. D.; Rolison, D. R.; Sankey, O.; Schanze, K. S.; Yardley, J.; Zhu, X. *J. Phys. Chem. B* **2003**, *107*, 6668–6697.

10.1021/ic701220t CCC: $40.75
Published on Web 09/29/2007

π-conjugated organic units of variable length. Such systems are particularly amenable for experimental and theoretical studies focused on issues related to charge and exciton structure and delocalization in linear π-conjugated organic systems.[16–20]

While there have been a number of experimental and theoretical reports concerning the properties of linear carbon chains and related structures, most of this work focused on vibrational and optical absorption spectroscopy.[5,13,18–20] Although several studies have reported fluorescence emission from carbon chain structures, there are only a few reports concerning the phosphorescence of oligoynes.[19,20] In an effort to increase the stability of linear carbon chain compounds, as well as extend the study of their photophysics to the triplet state, transition metals have been incorporated as end-caps to the oligoyne chains.[12,14] Notable examples of this work include a spectroscopic study of two- and four-carbon chains spanning two gold atoms reported by Che and co-workers[21] and a spectroscopic study of a series of platinum(II)−terpyridyl-capped carbon chains reported by Yam and co-workers.[22] Both of these studies provide evidence that the heavy metal end-groups induce efficient population of a $^3\pi,\pi^*$ state that is localized on the carbon chain. The triplet is clearly distinguished by its characteristic phosphorescence emission, which appears as a well-defined vibronic progression with spacing of ca. 2100 cm^{-1}.

One of our groups has developed synthetic methods that allow routine construction of variable-length carbon chains capped on both ends by transition metal units. In particular, we have recently reported the synthesis and structural characterization of an extensive series of linear carbon chain oligomers of the type Ar−Pt(P_2)−$(C{\equiv}C)_n$−Pt(P_2)−Ar, where Ar = aryl, P = a phosphine ligand, and n = 2–14.[10,11] The structural, optical, and electronic properties of these oligomers have been probed by X-ray crystallography, UV−visible absorption, and density functional theory (DFT) calculations.[11,16] While the optical and theoretical investigations provide considerable insight concerning electronic structure and π-conjugation in the carbon chains, little work has been done previously to probe the structure and dynamics of the long-lived excited states (e.g., singlet and/or triplet excitons) in the oligoyne systems.

In the present article we report a detailed study of the photophysics of the series of platinum end-capped oligoynes, **PtC_xPt** (x = 6, 8, 10, 12; Chart 1). This study has focused on the properties of the $^3\pi,\pi^*$ state localized on the carbon chains that span the two platinum centers. The triplet state is produced in relatively high yield in these oligoynes due to the strong spin−orbit coupling induced by the platinum centers. The spectroscopy and dynamics of the triplet state are probed using variable-temperature luminescence, transient absorption, and time-resolved emission spectroscopy. The results provide clear evidence for an energy gap law dependence of the nonradiative decay rate of the triplet state.

Chart 1

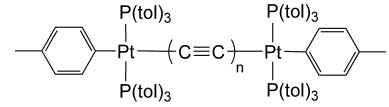

PtC_xPt x = 6, 8, 10, 12
x = 2n
tol = p-tolyl-

Experimental Section

Photophysical Measurements. Steady-state absorption measurements were recorded on a Varian Cary 100 dual-beam spectrophotometer. Corrected steady-state emission measurements were conducted on a SPEX Fluorolog-3 spectrophotometer. All sample solutions were prepared in tetrahydrofuran (THF) or 2-methyltetrahydrofuran (MTHF). Solvents were distilled from CaH_2 immediately prior to use. Room-temperature measurements were carried out in 1-cm square quartz cuvettes, and sample concentrations were adjusted such that the solutions were optically dilute (A_{max} < 0.20). Low-temperature emission measurements were conducted in 1-cm diameter borosilicate glass tubes in a liquid-nitrogen-cooled Oxford Instruments OptistatDN cryostat connected to an Omega CYC3200 autotuning temperature controller. For optical measurements at room temperature, solutions were deoxygenated by purging with argon for 30 min. For low-temperature measurements in the cryostat, degassing was accomplished by three consecutive freeze−pump−thaw cycles on a high-vacuum (10^{-5} Torr) line.

Photoluminescence quantum yields were determined by relative actinometry, with $Ru(bpy)_3^{2+}$ as an actinometer (ϕ_p = 0.055 in water). Low-temperature quantum yields were calculated by appropriately scaling the integrated emission area with temperature.[23]

The phosphorescence spectra for **PtC_6Pt**, **PtC_8Pt**, and **$PtC_{10}Pt$** at 100 K were fitted using a single-mode Franck−Condon expression,[23,24]

$$I(\bar{\nu}) = \sum_{\nu_m=0}^{5}\left\{\left(\frac{E_{00}-\nu_m\hbar\omega_m}{E_{00}}\right)^3\frac{(S_m)^{\nu_m}}{\nu_m!}\exp\left[-4\ln 2\left(\frac{\bar{\nu}-E_{00}+\nu_m\hbar\omega_m}{\Delta\bar{\nu}_{0,1/2}}\right)^2\right]\right\} \quad (1)$$

where $I(\bar{\nu})$ is the relative emission intensity at energy ν, E_{00} is the energy of the 0−0 transition, ν_m is the quantum number of the average medium-frequency vibrational mode, $\hbar\omega_m$ is the average medium-frequency acceptor mode coupled to the triplet-excited-state to ground-state transition, S_m is the Huang−Rhys factor, and $\Delta\bar{\nu}_{0,1/2}$ is the half-width of the individual vibronic bands. The fits of the experimental emission spectra to eq 1 were carried out by using a Visual Basic macro in Microsoft Excel (a copy of the Excel spreadsheet is provided as Supporting Information). Equation 1 is programmed into the macro/spreadsheet, and it provides the

(16) Zhuravlev, F.; Gladysz, J. A. *Chem.−Eur. J.* **2004**, *10*, 6510–6522.
(17) Yang, S.; Kertesz, M. *J. Phys. Chem. A* **2006**, *110*, 9771–9774.
(18) Yang, S.; Kertesz, M.; Zolyomi, V.; Kuerti, J. *J. Phys. Chem. A* **2007**, *111*, 2434–2441.
(19) Nagano, Y.; Ikoma, T.; Akiyama, K.; Tero-Kubota, S. *J. Chem. Phys.* **2001**, *114*, 1775–1784.
(20) Nagano, Y.; Ikoma, T.; Akiyama, K.; Tero-Kubota, S. *J. Am. Chem. Soc.* **2003**, *125*, 14103–14112.
(21) Che, C.-M.; Chao, H.-Y.; Miskowski, V. M.; Li, Y.; Cheung, K.-K. *J. Am. Chem. Soc.* **2001**, *123*, 4985–4991.
(22) Yam, V. W.-W.; Wong, K. M.-C.; Zhu, N. *Angew. Chem., Int. Ed.* **2003**, *42*, 1400–1403.
(23) Caspar, J. V. Excited State Decay Processes in Osmium(II), Ruthenium(II) and Rhenium(I) Polypyridyl Complexes. Ph.D. Dissertation, University of North Carolina, Chapel Hill, NC, 1982.
(24) Whittle, C. E.; Weinstein, J. A.; George, M. W.; Schanze, K. S. *Inorg. Chem.* **2001**, *40*, 4053–4062.

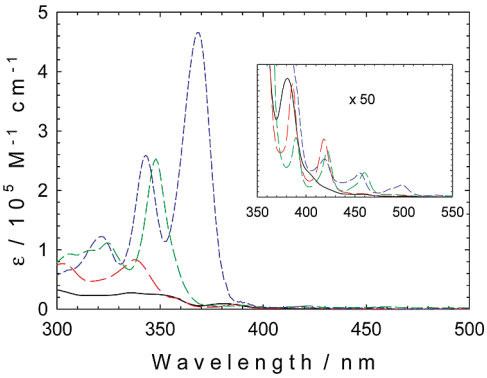

Figure 1. Absorption spectra of **PtC$_x$Pt** complexes in THF solution. In order of increasing molar absorptivity: $x = 6$, 8, 10, and 12. The inset shows the long-wavelength region of the spectra with expanded y scale (inset y scale range: 0–10 000 M^{-1} cm^{-1}).

capability for the user to input the four fitting parameters E_{00}, $\hbar\omega_m$, S_m, and $\Delta\bar{\nu}_{0,1/2}$. The experimental spectrum is input into the spreadsheet, and the fit is carried out by manually adjusting the four parameters until the best fit is obtained (by visual inspection). Typically, E_{00} and $\hbar\omega_m$ are first optimized and then S_m and $\Delta\bar{\nu}_{0,1/2}$ are adjusted to "fine-tune" the fit. Due to the well-defined nature of the vibrational progression in the experimental spectra of **PtC$_6$Pt**, **PtC$_8$Pt**, and **PtC$_{10}$Pt**, there is little "cross-correlation" between the fitting parameters.

Time-resolved emission measurements were carried out on a home-built apparatus consisting of a Continuum Surelite series Nd:YAG laser as the excitation source ($\lambda = 355$ nm, 10 ns fwhm, <1 mJ/pulse) and detection measured with a Princeton Instruments PI-MAX intensified CCD camera detector coupled to an Acton SpectraPro 150 spectrograph. Lifetimes were calculated by using global analysis of the spectral-kinetics data using the SPECFIT/32 software package (Biologic SAS, Grenoble, France, www.bio-logic.info).

Transient absorption measurements were conducted on a previously described home-built apparatus.[25] Samples were contained in a cell with a total volume of 10 mL, and the contents were continuously circulated through the pump−probe region of the cell. Solutions were deoxygenated by argon purging for 40 min and concentrations adjusted so that $A_{355} \approx 0.8$. Excitation was generated using the third harmonic output of a Nd:YAG laser (Spectra Physics GCR-14). Typical excitation energies were 5 mJ/pulse, corresponding to an irradiance of ca. 20 mJ/cm^2. Transient absorption spectra and decay lifetimes were generated by using software developed in-house.

Results

UV−Vis Absorption Spectra. The absorption spectra for the series of **PtC$_x$Pt** oligomers in CH_2Cl_2 have recently been reported.[11] However, to facilitate comparison with the photophysical data presented herein, the absorption spectra of the series were measured in THF and the results are presented in Figure 1. The spectra in THF solution are nearly identical to those reported in CH_2Cl_2;[11] however, the molar absorptivity values are slightly larger in THF. In each case, the absorption spectra of the oligoynes feature two primary transitions which each appear as a well-defined vibronic progression that shifts to lower energy with increasing carbon chain length. The low-energy transition (band I) is comparatively weak ($\epsilon < 5000$ M^{-1} cm^{-1}), whereas the higher-energy transition (band II) is considerably more intense, with the molar absorptivity increasing with carbon chain length. On the basis of DFT computations, both of these bands are assigned as arising from π,π^* transitions between orbitals that are concentrated on the $-(C{\equiv}C)_n-$ chains.[16]

(25) Wang, Y.; Schanze, K. S. *Chem. Phys.* **1993**, *176*, 305–19.

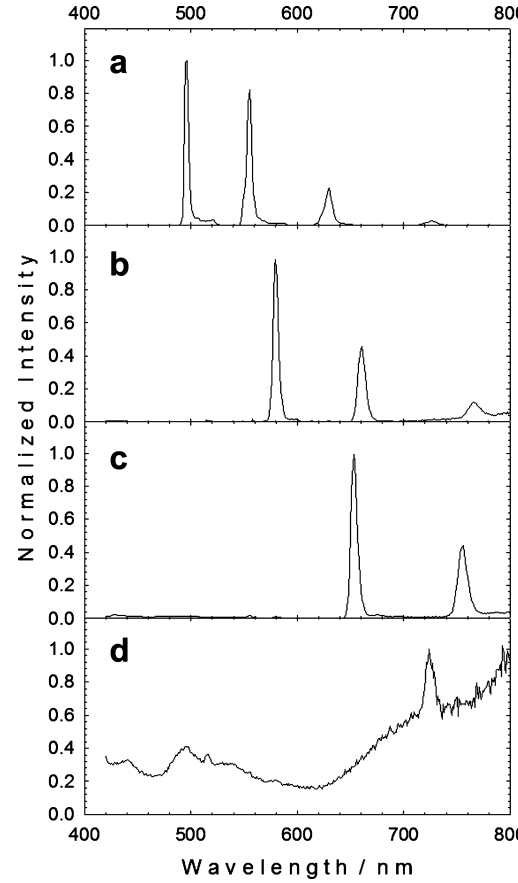

Figure 2. Photoluminescence spectra of **PtC$_x$Pt** complexes in 2-MTHF solvent glass at 80 K. (a) **PtC$_6$Pt**, $\lambda_{ex} = 335$ nm. (b) **PtC$_8$Pt**, $\lambda_{ex} = 335$ nm. (c) **PtC$_{10}$Pt**, $\lambda_{ex} = 350$ nm. (d) **PtC$_{12}$Pt**, $\lambda_{ex} = 368$ nm. The sloping background in (d) for $\lambda > 600$ nm is due to the correction factors which magnify the small background (dark count) signal at longer wavelengths where the detector response is lowest.

Steady-State Photoluminescence Spectroscopy. Photoluminescence spectra for all of the **PtC$_x$Pt** complexes were studied in MTHF solution at temperatures ranging from 300 to 80 K over the wavelength interval 400–800 nm. (The low-energy limit in the spectra is determined by the falloff in the photomultiplier detector response.) As shown in Figure 2, at 80 K in the MTHF glass the C_6, C_8, and C_{10} oligomers display a well-defined photoluminescence that can be assigned to phosphorescence from a $^3\pi,\pi^*$ excited state. (Fluorescence can be discerned in the region $\lambda = 450$–550 nm for the C_8, C_{10}, and C_{12} complexes, but the intensity is so weak that analysis of the spectra was not possible.) The emission from the C_{12} complex is very weak; however, the origin of the phosphorescence can be discerned in the far-red region of the visible. (The spectra shown in Figure 2 were obtained with excitation at the absorption maximum for each complex; however, the observed emission spectra did not vary with excitation wavelength.) For the C_6, C_8, and C_{10} oligomers, the phosphorescence appears as a narrow

Table 1. Emission Spectral Fitting Parameters for **PtC$_x$Pt** Complexes at 100 K

	$\lambda_{max,em}$	E_{00}/cm^{-1}	$\hbar\omega$/cm^{-1}	$\Delta\nu_{0,1/2}$/cm^{-1}	S_m	ΔE_{ST}/eV
C6	497	20 121	2150	190	1.05	0.53
C8	580	17 241	2120	200	0.90	0.71
C10	657	15 221	2060	250	0.78	0.75
C12	727	13 755	2020[a]	260[a]	0.71[b]	0.68

[a] Estimated values. [b] Estimated from linear plot of S_m vs E_{00}.

0−0 band followed by a series of vibronic sub-bands at lower energy separated by ca. 2100 cm^{-1}. The 0−0 bands of the phosphorescence red-shift systematically with increasing carbon chain length, and the λ_{max} value for the phosphorescence origin for each complex is listed in Table 1. The vibronic progression in each spectrum arises due to coupling of the triplet excitation to the C≡C stretch of the carbon chain. For **PtC$_6$Pt** the 0−1, 0−2, and 0−3 sub-bands are resolved, for **PtC$_8$Pt** the 0−1 and 0−2 sub-bands are seen, and for **PtC$_{10}$Pt** only the 0−1 sub-band appears in the accessible spectral range. The phosphorescence of **PtC$_{12}$Pt** is weaker than for the other oligomers, and it is so red-shifted that it is only possible to observe the origin of the phosphorescence.

While the vibrational progression in the phosphorescence is dominated by the 2100 cm^{-1} mode, the phosphorescence spectra of the C_6, C_8, and C_{10} oligomers also show evidence for weak coupling to lower-frequency modes ($\hbar\omega$ < 1000 cm^{-1}). In particular, a weak-intensity emission can be seen on the red side of the primary vibronic emission bands. This emission is most pronounced in the C_6 oligomer on the red side of the 0−0 band, but it can also be discerned in the spectra of the other oligomers. The weak-intensity, low-frequency progression may arise from coupling of the excitation to carbon-chain bending modes or modes associated with the aryl rings at the end of the platinum-capped carbon chains.

With increasing temperature, the phosphorescence spectra change little in energy or band shape; however, the emission intensity steadily decreases (see Figure S-1 in the Supporting Information). The emission from all of the complexes is much weaker at ambient temperature (300 K), and for **PtC$_6$Pt** and **PtC$_{12}$Pt**, the phosphorescence is too weak to detect at 300 K. The room-temperature phosphorescence quantum yields were measured for **PtC$_8$Pt** and **PtC$_{10}$Pt** (0.003 and 0.0012, respectively). Using these values, the phosphorescence quantum yields at 100 K were estimated by scaling the room-temperature quantum yields by the integrated emission area (which increases with decreasing temperature). These extrapolated low-temperature quantum yields are 0.018 and 0.0053 for **PtC$_8$Pt** and **PtC$_{10}$Pt**, respectively. Because there was no phosphorescence at ambient temperature for **PtC$_6$Pt** and **PtC$_{12}$Pt**, the low-temperature emission quantum yields could not be determined.

Fluorescence–excitation spectra obtained for each of the complexes while monitoring the phosphorescence at 80 K are shown in the Supporting Information (Figure S-2). In general, the excitation spectra are closely similar to the absorption spectra, except the bands are better resolved due to the low-temperature glass.

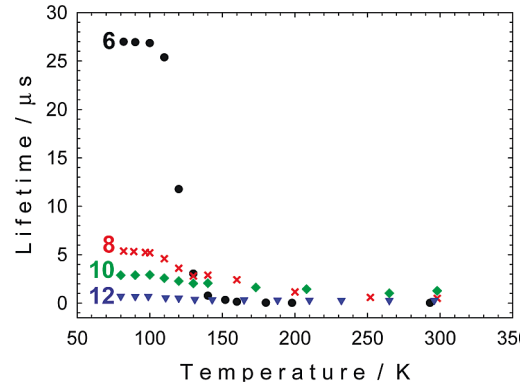

Figure 3. Temperature dependence of photoluminescence decay lifetimes for **PtC$_x$Pt** complexes in MTHF solution (glass). Carbon chain length (x) indicated in plot.

In order to provide more information concerning the nature of the triplet state that gives rise to the phosphorescence, the low-temperature (100 K) emission spectra of **PtC$_6$Pt**, **PtC$_8$Pt**, and **PtC$_{10}$Pt** were simulated by using a Franck−Condon band-shape analysis according to eq 1.[23,24] (The spectrum of **PtC$_{12}$Pt** could not be so treated since only the origin is observed.) The spectral simulations provide estimates for the 0−0 energy (E_{00}, the triplet energy), the frequency of the dominant vibrational mode coupled to the excitation ($\hbar\omega$), the bandwidth ($\Delta\bar{\nu}_{1/2}$), and the Huang−Rhys parameter (S_m) which is a quantitative measure of the geometric distortion between the ground and triplet excited states. A listing of the parameters recovered from the spectral simulations is shown in Table 1, and an example of the excellent quality of the fit of the experimental spectra is provided in Figure S-3 in the Supporting Information.

Several features are of interest with respect to the parameters recovered from the spectral fits. First, as noted above, E_{00} decreases systematically with increasing carbon chain length, reflecting the decrease in triplet energy with increasing length of the π-conjugated electron system. Second, as noted above, it is evident that the triplet excitation is coupled predominantly to a high-frequency vibration that corresponds to the stretching mode of the carbon chain. Interestingly, the frequency of the mode decreases slightly with increasing oligomer length, consistent with previous theoretical studies which indicate that the oligoyne stretching mode decreases in frequency with length.[18] Third, it is quite evident that the Huang−Rhys parameter decreases with increasing oligomer length (vide infra). This is consistent with the triplet exciton becoming more delocalized as the number of carbons in the sp chain increases.

Phosphorescence Decay Kinetics: Radiative and Nonradiative Decay Rates. Variable-temperature time-resolved emission spectra were measured for the **PtC$_n$Pt** series in degassed MTHF solution (glass) over the 80–300 K temperature range. The decay lifetimes recovered from fits of the emission decays are plotted vs temperature in Figure 3. Several features are of interest with respect to the temperature-dependent lifetimes. First, for all of the complexes the emission lifetimes decrease with increasing temperature. This lifetime decrease is especially large in the temperature region corresponding to the glass-to-fluid transi-

Table 2. Photophysical Parameters for **PtC$_x$Pt** Complexes

	$\tau_T/10^{-6}$ s[a]	ϕ_p[b]	ϕ_p[c]	$\phi_{isc}k_r/10^3$ s^{-1} [a]	$k_{nr}/10^3$ s^{-1} [a]	τ/μs[d]
C6	26.85	*e*	–	–	37.2	1.20
C8	5.24	0.003	0.018	3.44	187	1.41
C10	2.92	0.0012	0.0053	1.82	341	1.20
C12	0.54	*e*	–	–	1850	1.47

[a] Phosphorescence decay measured at 100 K. [b] Measured at room temperature (ca. 25 °C). [c] Extrapolated to 100 K; see text. [d] Extracted from room-temperature transient absorption. [e] Not observed.

tion of MTHF (120–140 K). Specifically, for **PtC$_6$Pt**, the lifetime decreases by nearly a factor of 20 between 110 and 150 K. For the other complexes, the decrease in lifetime is less, but nevertheless it is evident. Second, below the glass point of the solvent (e.g., $T = 100$ K) the emission lifetime increases with decreasing carbon chain length. For example, at 100 K, the emission lifetime increases by approximately a factor of 3 between **PtC$_{12}$Pt**, **PtC$_{10}$Pt**, and **PtC$_8$Pt** and then it increases by a further factor of 5 for **PtC$_6$Pt**. As discussed in more detail below, the overall trend of increasing triplet lifetime with decreasing chain length arises due to the energy gap law (vide infra).

By using the emission quantum yield and lifetime data at low temperature, it is possible to estimate the radiative and nonradiative decay rate constants (k_r and k_{nr}, respectively). The triplet lifetime (τ_T), phosphorescence quantum yield (ϕ_p), and intersystem crossing efficiency (ϕ_{isc}) are related to k_r and k_{nr} by the following expressions:

$$\tau_T = 1/(k_r + k_{nr}) \quad (2)$$

$$\phi_p = \phi_{isc} k_r \tau_T \quad (3)$$

Equations 2 and 3 can be rearranged to expressions that allow k_{nr} and k_r to be computed directly from the experimental parameters:

$$k_{nr} = \left[1 - \left(\frac{\phi_p}{\phi_{isc}}\right)\right]\frac{1}{\tau_T} \quad (4)$$

$$k_r = \left(\frac{\phi_p}{\phi_{isc}}\right)\frac{1}{\tau_T} \quad (5)$$

In order to apply these expressions to compute k_r and k_{nr}, values of τ_T, ϕ_p, and ϕ_{isc} are needed, but we note that ϕ_p is only known with certainty for two of the complexes and ϕ_{isc} is not known. However, given that the fluorescence is weak in all of the complexes and the observation of relatively strong triplet−triplet absorption, it is likely that ϕ_{isc} is significantly larger than 0.1, and for the shorter oligomers, it is likely close to unity. Thus, it is safe to conclude that $\phi_p \ll \phi_{isc}$ and eq 4 reduces to eq 6. We further rearrange eq 5 to the usable form eq 7, which emphasizes that there is some uncertainty in the computed radiative rate constants.

$$k_{nr} = \frac{1}{\tau_T} \quad (6)$$

$$\phi_{isc} k_r = \frac{\phi_p}{\tau_T} \quad (7)$$

The values of k_{nr} and $\phi_{isc}k_r$ computed from the experimental data at 100 K are listed in Table 2. Several features are of note with respect to this data. First, for **PtC$_8$Pt** and

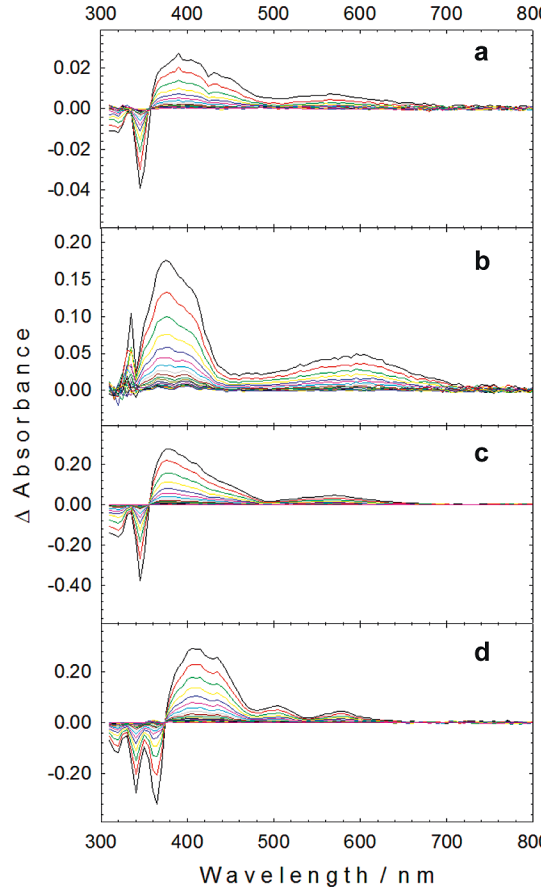

Figure 4. Transient absorption spectra of **PtC$_x$Pt** complexes following pulsed excitation with a 355 nm pulse (10 ns, 5 mJ/pulse): (a) **PtC$_6$Pt**, (b) **PtC$_8$Pt**, (c) **PtC$_{10}$Pt**, and (d) **PtC$_{12}$Pt**. For (a–c), the first spectrum was obtained at 20 ns following excitation, and subsequent spectra at 400 ns delay increments. For (d), the first spectrum was obtained at 20 ns following excitation, and subsequent spectra at 80 ns delay increments

PtC$_{10}$Pt, k_{nr} exceeds $\phi_{isc}k_r$ by nearly 100-fold, which indicates that the oligoynes decay predominantly via nonradiative pathway(s), even in the low-temperature glass. Second, it is evident that there is a systematic increase in k_{nr} with increasing carbon chain length. As noted above, this trend is a manifestation of the energy gap law. Finally, while there is limited data, it is also interesting that $\phi_{isc}k_r$ decreases from **PtC$_8$Pt** to **PtC$_{10}$Pt**; this effect probably arises because spin−orbit coupling induced by the Pt centers decreases with increasing chain length.

Transient Absorption Spectroscopy: Triplet−Triplet Absorption of the Oligoynes. In order to provide additional data concerning the properties of the triplet state of the oligoynes, nanosecond transient absorption spectra were measured at room temperature in deoxygenated THF solution. As shown in Figure 4, near-UV excitation of all of the complexes produces strongly absorbing transients which decay on a time scale of a few microseconds (computed decay lifetimes are listed in Table 2). The transient which gives rise to the absorption is the triplet excited state. In each case the transient difference-absorption spectra are characterized by bleaching of the near-UV ground-state absorption bands, combined with moderately intense triplet−triplet absorption in the visible region. Interestingly, for each complex, the triplet−triplet absorption appears to arise in

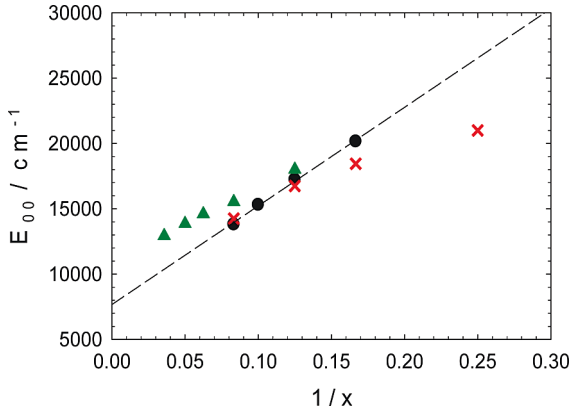

Figure 5. Correlation of E_{00} (triplet energy) vs $1/x$ for π-conjugated oligomers, where x = no. of carbons in the chain. (●) **PtC$_x$Pt** complexes. (×) Ph−(C≡C)$_n$−Ph oligomers (where $n = x/2$, from ref 8). (▲) α-Thiophene oligomers (from ref 27). The dashed line is the best fit to the **PtC$_x$Pt** data with $R^2 = 0.997$.

two distinct bands: one stronger band which is in the near-UV and blue of the visible and a second weaker band that is centered in the midvisible. (For **PtC$_{12}$Pt** the visible band is apparently split into vibronic bands.) While assignment of these transitions will require further (theoretical) study, it is evident from the transient absorption study that intersystem crossing is efficient in all of the oligoynes. Furthermore, it is clear that the triplet−triplet absorption of the carbon chains is strongly allowed. (These conclusions are based on the fact that for most of the complexes the observed ΔA values are considerable, i.e., >0.1 OD unit. Given that the ground-state concentration in the transient absorption solution is 10^{-5} M, assuming that the laser pulse is saturating, $\phi_{isc} = 1$ and ϵ_{TT} of 10^4 M^{-1} cm^{-1} are required to obtain $\Delta A = 0.1$.)

Discussion

Variation of Triplet Energy with Carbon Chain Length. One key result of the above data is that it provides the 0−0 triplet energy as a function of oligoyne chain length for the **PtC$_x$Pt** complexes. In order to analyze the chain-dependent triplet energy data, we have constructed the correlation in Figure 5, which shows a plot of E_{00} vs $1/x$, where x is the number of carbon atoms in the oligoyne chain. Interestingly, this plot features an excellent linear correlation and it provides an intercept of 7670 cm^{-1} (0.95 eV) which corresponds to the triplet energy in the −(C≡C)$_n$− polymer. It is noteworthy that there is substantial variation of the triplet energy across the **PtC$_x$Pt** series, a fact which implies that the triplet state is delocalized across the entire π-conjugated system defined by the carbon chain for all members of the **PtC$_x$Pt** series. There is no sign of leveling off of the triplet energy with increasing chain length, suggesting that for chains longer than C_{12} the triplet energy will continue to decrease (i.e., the effective "conjugation length" for the triplet has not been reached in this series).

In a recent study, Nagano and co-workers reported the evolution of the absorption, fluorescence, and phosphorescence of the series of diphenyl end-capped oligoynes Ph−(C≡C)$_n$−Ph (n = 1–6).[19,20] Using their reported phosphorescence 0−0 band energies, we have included their data in Figure 5 for comparison with that of the **PtC$_x$Pt** series. Interestingly, the correlation of E_{00} vs $1/x$ defined by the Ph−(C≡C)$_n$−Ph series is curved. For the shorter oligoynes, the trend defined by the Ph−(C≡C)$_n$−Ph series deviates (to lower energy) relative to the correlation for the **PtC$_x$Pt** series; however, for longer carbon chain length (n = 4 and 6) the data for Ph−(C≡C)$_n$−Ph series nearly converge to the correlation defined by the **PtC$_x$Pt** series. The curvature in the correlation for the Ph−(C≡C)$_n$−Ph series likely results from the fact that, for short oligoyne chain length, the triplet is delocalized significantly into the phenyl end-groups. (This hypothesis is supported by the observation of significant vibronic coupling to phenyl-based modes in the phosphorescence spectra of Ph−C≡C−Ph and Ph−(C≡C)$_2$−Ph.)[19] At longer chain length, the effect of the phenyl end-groups on the triplet energy in the Ph−(C≡C)$_n$−Ph series becomes less pronounced, and consequently, the two correlations converge. This comparison suggests that correlation of E_{00} vs $1/x$ for the **PtC$_x$Pt** series more accurately reflects the trend in triplet state energy for the "pure" −(C≡C)$_n$− carbon chain (i.e., without interference from the end-groups). Importantly, this comparison also shows that the triplet energy for the −(C≡C)$_n$− polymer that is extrapolated from the correlation for the **PtC$_x$Pt** series is likely a much better estimate than would be obtained from the Ph−(C≡C)$_n$−Ph series.

A number of recent studies have explored the variation of the singlet and triplet energies with oligomer length for π-conjugated oligomers such as oligothiophene,[26–29] oligo(phenylene vinylene)[30,31] and oligo(fluorene).[32] Of particular relevance to the present work are studies of thiophene and substituted thiophene oligomers, where very clear correlations of excited-state energy with oligomer length emerge.[26–28,32] Figure 5 also includes E_{00} values for the triplet state in the series of α-oligothiophene oligomers (for n = 2–7) reported by de Melo and co-workers.[27] In the plot the oligothiophene triplet energies are plotted vs $1/x$, where x is the number of carbon atoms in the π-conjugated chain (there are four carbons per thiophene repeat unit). Interestingly, it is clear that the trend of E_{00} vs $1/x$ for the oligothiophene series runs nearly parallel to the correlation defined by the **PtC$_x$Pt** series. This agreement indicates that the degree of triplet delocalization is similar in oligoynes compared to the oligothiophenes. Note, however, that the extrapolated value of the triplet energy for polythiophene is ca. 2500 cm^{-1} higher than that of the −(C≡C)$_n$− polymer.

Since significant fluorescence was not observed for the **PtC$_x$Pt** series, it is only possible to estimate the S_1 energy

(26) Becker, R. S.; de Melo, J. S.; Macanita, A. L.; Elisei, F. *J. Phys. Chem.* **1996**, *100*, 18683–18695.
(27) de Melo, J. S.; Silva, L. M.; Arnaut, L. G.; Becker, R. S. *J. Chem. Phys.* **1999**, *111*, 5427–5433.
(28) Wasserberg, D.; Marsal, P.; Meskers, S. C. J.; Janssen, R. A. J.; Beljonne, D. *J. Phys. Chem. B* **2005**, *109*, 4410–4415.
(29) Wasserberg, D.; Meskers, S. C. J.; Janssen, R. A. J.; Mena-Osteritz, E.; Bäuerle, P. *J. Am. Chem. Soc.* **2007**, *128*, 17007–17017.
(30) Martin, R. E.; Diederich, F. *Angew. Chem., Int. Ed.* **1999**, *38*, 1351–1377.
(31) Candeias, L. P.; Wildeman, J.; Hadziioannou, G.; Warman, J. M. *J. Phys. Chem. B* **2000**, *104*, 8366–8371.
(32) Wasserberg, D.; Dudek, S. P.; Meskers, S. C. J.; Janssen, R. A. J. *Chem. Phys. Lett.* **2005**, *411*, 273–277.

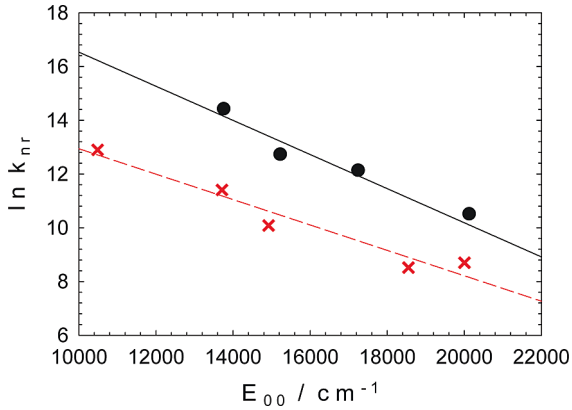

Figure 6. Energy gap law correlation; see text for details. (●) **PtC$_x$Pt** complexes. The solid line is best fit with $R^2 = 0.951$. (×) Platinum−acetylide oligomers (from ref 39). The dashed line is the best fit with $R^2 = 0.946$.

based on the onset of the absorption bands. Using this as an approximation for the S_1 state energy, we have computed estimated singlet−triplet splitting (ΔE_{ST}) for the **PtC$_x$Pt** series, and the values are listed in Table 1. Interestingly, for the three longer oligoynes, the ΔE_{ST} cluster is around a value of 0.7 eV, which is in good accord with the value observed for a variety of other long π-conjugated systems, including poly(thiophene) and poly(phenylene vinylene).[33]

Energy Gap Law Correlation for the Oligoynes. The energy gap law was first suggested by Robinson and Frosch to explain the systematic variation of triplet-state nonradiative decay rates in polycyclic aromatic hydrocarbons.[34] Shortly thereafter, Siebrand developed a quantitative theory for the energy gap law.[35] The energy gap law predicts that the rate of nonradiative decay of an excited-state will increase as the excited-state energy decreases. The effect arises because of the relationship between the Franck−Condon factors (FCF) for vibrational overlap of the excited and ground electronic states and the energy gap (and geometric distortion) between the potential surfaces for the two electronic states (see below, eq 8a−8c). The most comprehensive study of the energy gap law carried out to date lies in the work of Meyer and co-workers who showed the existence of a quantitative relationship between excited-state energy and the nonradiative rate for the metal-to-ligand charge transfer state in a series of Ru(II) and Os(II) polypyridine complexes.[36–38] More recently, Köhler and co-workers showed that the energy gap law holds for triplet decay in a series of platinum−acetylide oligomers and polymers.[39]

A focus of the present investigation is to explore whether the energy gap law holds for decay of the triplet excited-state in the series of platinum end-capped oligoynes. This study is of interest due to the remarkable simplicity of the carbon chains: they consist of a linear, π-conjugated electronic system in which the excitation is coupled to a single, very well-defined high-frequency vibrational mode. In short, the oligoynes seem to provide an ideal platform to examine the correlation between spectroscopy, triplet energy, and nonradiative decay rate.

The following expressions provide the complete relationship between the nonradiative decay rate and parameters accessible from spectroscopy,[24,36]

$$\ln k_{nr} = \ln \beta_o - S_m + (\gamma_0 + 1)^2 \frac{(\Delta\bar{\nu}_{0,1/2}/\hbar\omega_m)_2}{16 \ln 2} - 0.5 \ln\left(\frac{\hbar\omega_m E_{00}}{1000\ \mathrm{cm}^{-1}}\right) - \frac{\gamma_0 E_{00}}{\hbar\omega_m} \quad (8a)$$

$$\beta_o = |C_k|^2 \omega_k \left(\frac{\sqrt{\pi/2}}{1000\ \mathrm{cm}^{-1}}\right) \quad (8b)$$

$$\gamma_0 = \ln\left(\frac{E_{00}}{\hbar\omega_m S_m}\right) - 1 \quad (8c)$$

where S_m, E_{00}, $\Delta\bar{\nu}_{0,1/2}$, and $\hbar\omega_m$ are the same terms defined in eq 1, β_o is the vibronically induced electronic coupling term, C_k is the vibronic coupling matrix element, and ω_k is the frequency of the promoting vibrational mode. These equations can be simplified in order to facilitate analysis of experimental data. The assumption that all terms on the right-hand side of eq 8a except the last one are independent of changes in E_{00} leads to eq 9a.[38] This equation predicts a linear relationship between the (natural) log of the nonradiative decay rate and E_{00}, with a slope equal to $\gamma_o/\hbar\omega$ (this is the mathematical statement of the energy gap law). Also, since $\ln \beta_o$ is the only term in eq 8a that cannot be computed using parameters derived from a Franck−Condon fit of an emission spectrum, this equation can be recast as eq 9b where ln[FCF(calcd)] is an abbreviation for "calculated FCF". Note that ln[FCF(calcd)] is computed by substituting the parameters recovered from the emission spectral fits (Table 1) into the last four terms on the right-hand side of eq 8a. The latter expression implies that a plot of ln[FCF(calcd)] vs $\ln k_{nr}$ will be a linear correlation with a slope equal to unity.

$$\ln k_{nr} = a - \left(\frac{\gamma_0}{\hbar\omega_m}\right) E_{00} \quad (9a)$$

$$\ln[\mathrm{FCF(calcd)}] = \ln k_{nr} - \ln \beta_o \quad (9b)$$

Figure 6 illustrates plots of $\ln k_{nr}$ vs E_{00} for the **PtC$_x$Pt** series (filled circles, values at 100 K; see Table 2). We have also included in the correlation data from the series of platinum−acetylide oligomers reported by Köhler.[39] Several features are evident from this presentation. First, the nonradiative decay rates for the **PtC$_x$Pt** series clearly follow the correlation predicted by the energy gap law. This result shows that in the frozen solvent glass nonradiative decay of the triplet state in the oligoynes is controlled by the extent of vibronic coupling of the exciton to the high-frequency mode (the −C≡C− stretch), which varies (exponentially) with the excited-state energy. The slope of the energy gap

(33) Köhler, A.; Wilson, J. S.; Friend, R. H.; Al-Suti, M. K.; Khan, M. S.; Gerhard, A.; Bassler, H. *J. Chem. Phys.* **2002**, *116*, 9457–9463.
(34) Robinson, G. W.; Frosch, R. P. *J. Chem. Phys.* **1963**, *38*, 1187–1203.
(35) Siebrand, W. *J. Chem. Phys.* **1967**, *47*, 2411–2422.
(36) Caspar, J. V.; Meyer, T. J. *J. Phys. Chem.* **1983**, *87*, 952–957.
(37) Kober, E. M.; Caspar, J. V.; Lumpkin, R. S.; Meyer, T. J. *J. Phys. Chem.* **1986**, *90*, 3722–3734.
(38) Barqawi, K. R.; Murtaza, Z.; Meyer, T. J. *J. Phys. Chem.* **1991**, *95*, 47–50.
(39) Wilson, J. S.; Chawdhury, N.; Al-Mandhary, M. R. A.; Younus, M.; Khan, M. S.; Raithby, P. R.; Köhler, A.; Friend, R. H. *J. Am. Chem. Soc.* **2001**, *123*, 9412–9417.

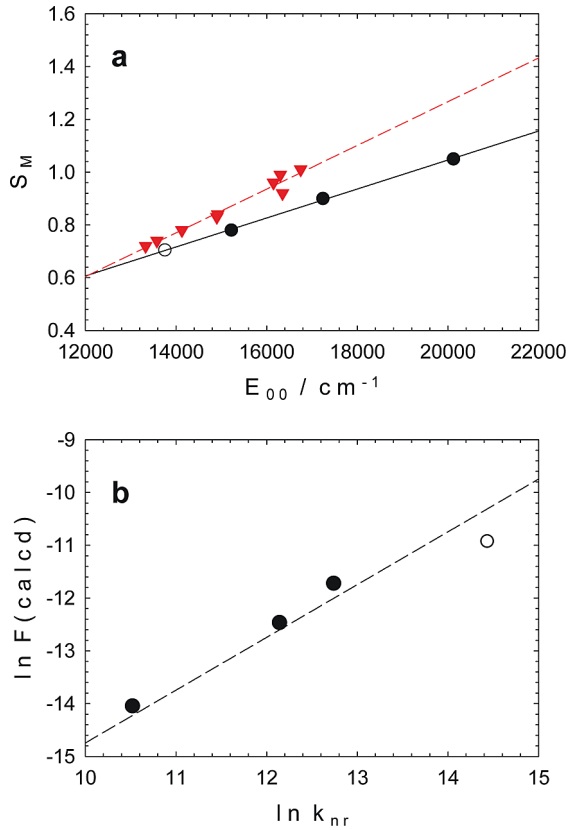

Figure 7. (a) Plot of the Huang−Rhys parameter (S_m) vs the triplet energy (E_{00}) for **PtC$_x$Pt** complexes (●) and for the series of ruthenium polypyridyl complexes (▼). Data for the ruthenium complexes are from ref 38. Lines are the best fit to data, $R^2 = 0.999$ for **PtC$_x$Pt** complexes and $R^2 = 0.963$ for ruthenium polypyridyl complexes. (b) Plot of calculated Franck−Condon factors vs natural log of the nonradiative rate for **PtC$_x$Pt** complexes. The line has a slope of unity. In both plots, the open circle data point (○) is for **PtC$_{12}$Pt**. The S_m value for **PtC$_{12}$Pt** in plot (a) is extrapolated using the best fit line ($R^2 = 0.960$) and the experimental E_{00} value, and the ln F(calcd) value for this complex in plot (b) is computed using the extrapolated S_m value.

correlation for the **PtC$_x$Pt** series is almost the same as that defined by the platinum−acetylide oligomers reported by Köhler.[39] This correspondence in the energy gap law dependence likely arises because in both of the platinum-containing systems the −C≡C− stretching mode is likely the dominant acceptor mode coupled to nonradiative decay. The correlation for the **PtC$_x$Pt** series has a larger intercept value, which reflects the fact that nonradiative decay is faster at equal excited-state energy in the two series. This larger "intrinsic" k_{nr} (a in eq 9a) for the **PtC$_x$Pt** series may be due to the fact that in the platinum−acetylides studied by Köhler medium-frequency modes (aromatic ring C−C stretching) are also coupled to the triplet exciton. This would effectively decrease the FCF for nonradiative decay (note that ω_k appears in the β_o term in eq 8a).

Also of interest is the correlation of the Huang−Rhys parameter (S_m, calculated from the fits of the emission spectra of the **PtC$_x$Pt** oligomers for $n = 6$, 8, and 10, values in Table 1) with the triplet energy shown in Figure 7a. As can be seen from this correlation, S_m decreases with E_{00}, with a very good linear correlation being defined by the series. (By extrapolating the linear correlation defined for **PtC$_6$Pt**, **PtC$_8$Pt**, and **PtC$_{10}$Pt**, we have estimated the S_m value for **PtC$_{12}$Pt**.) The decrease in S_m with increasing carbon chain length is consistent with the triplet excited-state becoming more delocalized, which has the effect of decreasing the electron-vibrational coupling. A similar correlation for S_m vs E_{00} was reported by Meyer for a metal-to-ligand charge transfer states in a series of Ru−polypyridine complexes, and these data are shown for comparison in Figure 7a.[38] Despite the significant difference in the nature of the excited states for the Ru−polypyridine and **PtC$_x$Pt** complexes (metal-to-ligand charge transfer and $^3\pi,\pi^*$, respectively), the correlations are remarkably similar.

Finally, as noted above, it is possible to compute the FCF for nonradiative decay using the parameters obtained from the emission fits. As suggested by eq 9b, the calculated FCF values should vary linearly with ln k_{nr}, with a slope of unity and a single adjustable parameter which corresponds to ln β_o.[24,38] Figure 7b shows the correlation of ln FCF and ln k_{nr}, where the ln FCF values for the **PtC$_x$Pt** complexes were computed using the parameters recovered from the spectral fits (Table 1) and eq 8a−8c. (Since it was not possible to fit the emission spectrum for **PtC$_{12}$Pt**, the S_m needed to compute ln FCF for this complex was extrapolated using the observed E_{00} value in the correlation shown in Figure 7a.) The dashed line in Figure 7b has a slope of unity and an intercept of −24.7, which affords a value of $\beta_o = 5.3 \times 10^{10}$ cm^{-1}. Given the relatively large range in E_{00} and k_{nr} values for the series (6000 cm^{-1} and a factor of 50), the correlation of the calculated FCF and the nonradiative decay rates is impressive. The quality of the correlation underscores the quality of the energy gap law correlation for the **PtC$_x$Pt** series, and that in the frozen solvent glass nonradiative decay is controlled by coupling to the −C≡C− mode of the carbon chain.

Excited State Decay above the Solvent Glass Point. As noted above, the energy gap correlation for the **PtC$_x$Pt** series holds only at temperatures below the solvent glass point. It is evident that in fluid solution an additional nonradiative decay pathway is active that dominates decay of the triplet state. Activation of this pathway as the glass melts is very evident in **PtC$_6$Pt**; for this complex, the lifetime decreases by nearly a factor of 100 as the temperature is increased from 100 to 160 K. Given that this decay pathway is activated by melting of the solvent matrix, it is reasonable to assume that it is related to the increase in the ability of the carbon chain to undergo fluxional motion. Previous theoretical and experimental studies of −(C≡C)$_n$− oligomers indicate that in some cases the optimum geometry in the excited-state involves a transoid conformation in which the triple bond length is significantly increased (i.e., the carbons atoms are better approximated as sp^2 hybridized).[19,40] Although there is insufficient experimental data from the present photophysical studies to prove that a bending mode of the −(C≡C)$_n$− chain is the origin of the accelerated triplet decay in fluid solution, we believe that it is a very reasonable hypothesis. Future DFT calculations which probe the geo-

(40) Ishibashi, T.; Hamaguchi, H. *J. Phys. Chem. A* **1998**, *102*, 2263–2269.

metric energy landscape for the triplet state of the **PtC$_x$Pt** series may provide insight into this issue.

Summary and Conclusions

A detailed photophysical investigation of a homologous series of carbon chain oligomers that are end-capped with bis(phosphine) aryl platinum units has been carried out. The photophysics of the complexes is dominated by a $^3\pi,\pi^*$ state that is concentrated on the $-(C{\equiv}C)_n-$ chain, and the triplet state is produced in comparatively high quantum yield due to the strong spin−orbit coupling induced by the platinum metal centers. At low temperature (T < 130 K), each of the complexes exhibits a unique, highly structured phosphorescence that is characterized by a series of narrow (<200 cm^{-1} fwhm) vibronic bands separated by ca. 2100 cm^{-1}. The appearance of the spectrum signals that the triplet state is coupled to a single, high-frequency vibrational mode that corresponds to the stretch of the $-(C{\equiv}C)_n-$ chain. Analysis of the phosphorescence spectra using a single-mode Franck−Condon band shape analysis indicates that the 0−0 energy of the triplet state decreases by ca. 6000 cm^{-1} as the length of the carbon chain increases from 6 to 12 atoms, and the electron-vibrational coupling constant (S_m) decreases with increasing chain length. At room temperature the triplet state can be observed by transient absorption spectroscopy, and each of the complexes exhibits moderately intense triplet−triplet absorption throughout the visible region (400–700 nm).

Phosphorescence lifetime studies were carried out on the series to study the decay kinetics of the triplet state. At low temperature in a frozen solvent glass, the triplet lifetime monotonically increases with decreasing length of the carbon chain, with the lifetimes ranging from 27 μs (**PtC$_6$Pt**) to 500 ns (**PtC$_{12}$Pt**). Given that the phosphorescence quantum yields are comparatively low, the lifetimes are controlled by the rate of nonradiative decay and the observed lifetime variation at low temperature is attributed to the energy gap law. Consistent with this hypothesis, the nonradiative decay rates of the complexes at T = 100 K are shown to exhibit a quantitative energy gap law correlation.

The properties of the triplet state in the **PtC$_x$Pt** series are believed to be minimally perturbed by the presence of the platinum complex end-capping units. Consequently, the results of this study provide the best available quantitative insight concerning the structure and dynamics of the triplet state in carbon chains of extended length.

Acknowledgment. We thank the National Science Foundation (CHE-0515066, K.S.S.; CHE-0719267, J.A.G.), the Deutsche Forschungsgemeinschaft (SFB 583, J.A.G.), and Johnson Matthey (platinum loan) for support of this research.

Supporting Information Available: Fitted phosphorescence emission spectrum of **PtC$_6$Pt**, temperature-dependent phosphorescence spectra of **PtC$_8$Pt**, emission excitation spectra for the **PtC$_x$Pt** series, and the Microsoft Excel spreadsheet used for emission spectral fits (three figures and one Microsoft.xls file). This material is available free of charge via the Internet at http://pubs.acs.org.

IC701220T